2016 IEEE/RSJ International Conference on Intelligent Robots and Systems (IROS)
Daejeon Convention Center
October 9-14, 2016, Daejeon, Korea

Machining with serial and quasi-serial industrial robots: comparison analysis and architecture limitations

A. Klimchik, E. Magid and A. Pashkevich

Abstract— **The paper deals with comparison study of serial and quasi-serial industrial robots used for machining operations. It proposes a new methodology for robot ranking, which is based on estimation of the end-effector resistance to cutting forces for several machining tasks, which are optimally located within the robot workspace. To cover wide range of applications, a set of isotropic, quasi-isotropic and extended benchmark tasks are considered. It is shown that regardless of the benchmark problem, seral manipulators are preferable for small and medium tasks while quasi-serial ones' better suit large-dimensional tasks. The proposed technique was applied for the comparison analysis of 10 industrial robots of both serial and quasi-serial architectures with similar working radius and payload of about 200 kg.**

Keywords— **Robot-based machining, serial vs. parallel, optimal task placement, industrial robot, stiffness model.**

I. Introduction

Current enhancement of robot performances increase robots applications areas from traditional pic-and-place and welding [1, 2], to machining where robotic manipulators are subjected to significant external loading caused by tool-workpiece interaction [3]. At present, robots rapidly take their niche in milling [4], friction stir welding [5, 6], drilling [7, 8] and other operations [9, 10], progressively replacing less flexible and more expensive CNC machines. Nevertheless, robot positioning accuracy under external loading remains rather limited, and practicing engineers face the problem of well-grounded robot selection from the big variety of industrial robots provided by manufactures. To help a final user, this paper proposes an engineering technique that deals with comparison of robot architecture and their basic parameters taking into account influence of the external loading, which is generated by a technological operation.

To improve robot accuracy under loading, there were developed different online and off-line methods [11-14], which allow to reduce an impact of manipulator deformations on machining quality. The most efficient technique is based on online tracking of robot position and compensation of related deflections [15]. This approach is able to compensate errors of different nature, but it requires expensive equipment like laser tracker and essentially limits working area because of reflector visibility. Another group of the on-line methods is based on information from internal robot sensors; they could be implemented relatively easily and usually do not impose any restriction to the robot workspace. However, these methods require rather accurate geometric and stiffness models of the manipulator, which should be obtained from the dedicated experimental study [16]. The most essential limitation of the on-line approach is related to necessity of the model modification in robot controller, which is usually not completely open for the end-user. In contrast, the off-line error compensation technique does not require any intervention into controller software and it is based on the target trajectory modification [17]. As follows from our experience, even simplified models are able to compensate about 80% of manipulator compliance errors [18], while a sophisticated complete model is able to compensate about 95% of the end-effector deformations [19].

Another trend to improve manipulator accuracy under the loading is based on mechanical methods, where the manipulator stiffness enhancement is achieved by means of closed loops, which transform conventional serial robots into quasi-serial ones. The most common way here is using gravity compensators, which do not affect essentially manipulator stiffness but reduce torque in actuated joints. An alternative way is to use kinematic parallelograms [20, 21], which potentially may improve robot stiffness. Moreover, even brief analyses showed that advantages of manipulators with kinematic parallelograms are not so evident. This poses a problem of comparison study and accuracy analysis of serial vs. quasi-serial manipulators for machining application.

To address this problem, it is required to develop dedicated performance measure that takes into account particularities of machining technologies. In classical robotics, robots are usually compared from point of view of their kinematic properties [22, 23]. However, these performance measures do not take into account robot elasticity and influence of external forces (applied to manipulator's end-effector) and thus do not suit well for evaluation of the manipulator performance under the external load. To overcome this difficulty, several other performance measures were developed that are based on the Cartesian stiffness matrix norms [24, 25] or manipulator deflections at the specific "test pose" [26, 27]. Nevertheless, they cannot be directly applied to robot architecture comparison for machining application since they ignore some important technological issues. For this reason, this paper proposes an industry oriented performance measure allowing to evaluate and to compare robot capabilities using criteria that are generally accepted in their area.

*The work presented in this paper was partially funded by Innopolis University and project FEDER ROBOTEX, France.

A. Klimchik and E. Magid are with Innopolis University, *Universitetskaya St, 1, Innopolis, 420500, Russia* (e-mail: a.klimchik@innopolis.ru, dr.e.magid@ieee.org).

A. Pashkevich is with Ecole des Mines de Nantes, 4 rue Alfred-Kastler, Nantes 44307, France and with Institut de Recherches en Communications et Cybernétique de Nantes (IRCCyN), 44321 Nantes, France (e-mail: anatol.pashkevich@mines-nantes.fr).

II. PROBLEM STATEMENT

A. Stiffness modeling of industrial robots

Typical serial manipulators contain three main components: robot base, robot arm and robot wrist (Fig. 1a). The robot base defines the arm orientation with respect to the robot world frame. The robot arm is responsible for major movements of the robot end-effector. For 6-dof non-redundant robots, the translational movements are usually realized using two actuated joints (the joints #2 and #3). Corresponding links #2 and #3 define manipulator workspace. The robot wrist provides orientation movements. In a relevant geometric model, the wrist linear parameters may be omitted and included in the parameters describing link #3 and tool transformation.

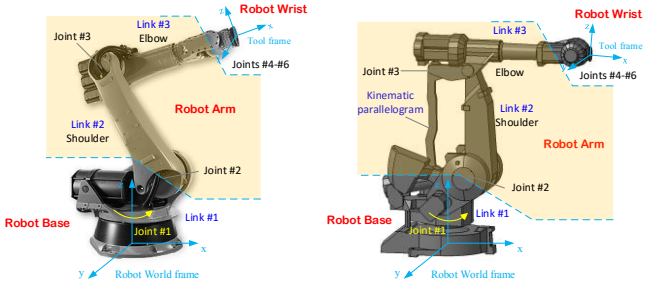

(a) typical serial manipulator (b) typical quasi-serial manipulator

Figure 1. Architecture of a typical industrial robot

Quasi-serial robots have roughly similar architecture (Fig. 1b). In contrast to strictly serial manipulators, a robot arm of a quasi-serial manipulator contains kinematic parallelogram, which can be treated as an internal closed-loop. For this reason, such robots are often called quasi-serial ones. In practice, the kinematic parallelogram allows robot designers to increase robot dynamic properties. Usually the parallelogram does not affect essentially manipulator control and does not change manipulator direct/inverse kinematic equations. On the other hand, the stiffness model of a quasi-serial manipulator essentially differs from its serial counterpart since the manipulator compliant element (actuator #3 transmission) re-location essentially influences the stiffness behavior [28]. For this reason, previous results obtained for strictly serial manipulators [18] cannot be used here directly.

Stiffness model of a robotic manipulator describes the manipulator behavior under loading [29]. In addition to the conventional robot parameters, it includes a number of elastic parameters describing flexibility of manipulator links and joints. In some industrial applications, the manipulator elasticity cannot be ignored since high loading is applied to the robot, while the required positioning accuracy is rather high. For example, according to our experience the end-effector deflection of heavy industrial robots under 1kN loading (typical loading in machining process) may vary from 1 to 10 mm within the robot workspace [30], while demanded accuracy for the machining process is about 0.1 mm. These compliance errors can be reduced to admissible level using both on-line and off-line error compensation techniques that are based on the appropriate stiffness model, either "complete" or "reduced". The complete stiffness model of an industrial robot is complicated, it takes into account the compliances of all manipulator links and actuators [19]. However, in practice, a number of manipulator components may be treated as rigid ones, while main compliance is concentrated in the actuator transmissions. This allows to apply so-called reduced models that take into account joint elasticities only [31]. In the majority of cases these models can be efficiently used to compare stiffness properties of manipulators. For this reason, the comparison study presented in this paper is based on the reduced stiffness model.

B. Motivation example and research problem

To define the research problem and to demonstrate advantages/disadvantages of both serial and quasi-serial architectures, let us present a motivation example showing that a proper manipulator type selection essentially depends on the technological task dimension and external force orientation. This example deals with two manipulators (serial and quasi-serial) with the same geometric parameters $l_2 = 1m$, $l_3 = 0.8m$ and joint compliances $k = 10^{-6}\ N\,m/rad$. These values are typical for industrial robots that are used in machining. To compare stiffness behavior, let us compute the compliance errors caused by an external force 1.0 kN applied to the end-effector. The relevant results have been obtained for two different forces. Figure 2 shows the compliance error distribution within the manipulator workspace: the elastostatic deflections vary from 0 to 3.83 mm for the serial manipulator and, from 0 to 1.62 mm for the quasi serial manipulator. The considered case study results show that the compliance errors range does not depend on the force direction, however the compliance error maps are essentially different.

To compare the considered architectures, let us first find the workspace point that provides the smallest compliance errors for all possible force directions. It is reasonable to locate a technological task of relatively small dimensions within the neighborhood of such point. The relevant computations show that the minimum compliance errors are 0.64 and 1.00 mm for the serial and quasi-serial architectures respectively (Fig. 3). Hence, the serial architecture is preferable for small-dimensional tasks.

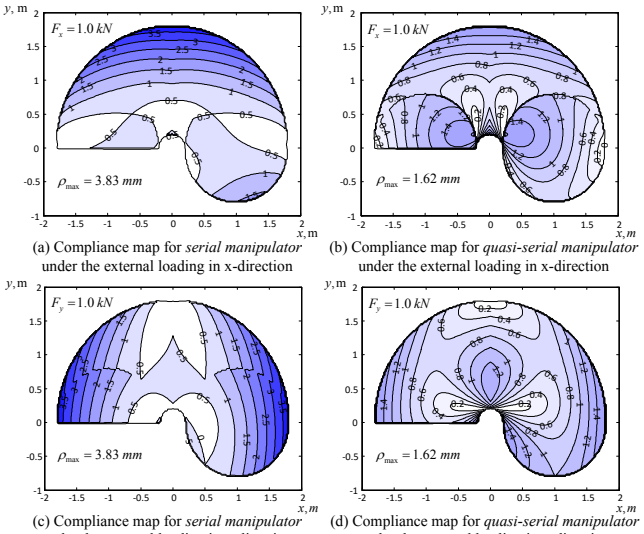

(a) Compliance map for *serial manipulator* under the external loading in x-direction

(b) Compliance map for *quasi-serial manipulator* under the external loading in x-direction

(c) Compliance map for *serial manipulator* under the external loading in y-direction

(d) Compliance map for *quasi-serial manipulator* under the external loading in y-direction

Figure 2. Compliance maps for serial (a,c) and quasi-serial (b,d) manipulators under different external loadings

Further, let us locate in the manipulator workspace a task of 0.5×2 m size, which can be treated as a large-dimensional one (with regard to the manipulator workspace. Corresponding computations show that the minimum compliance errors, which can be achieved for all possible force directions and for all task points are 1.8 mm and 1.4 mm for the serial and quasi-serial manipulators respectively. Hence, the quasi-serial architecture is preferable for large-dimensional tasks.

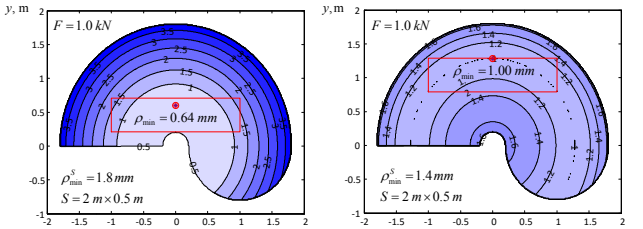

(a) Maximum compliance errors for arbitrary force directions for *serial manipulator*

(b) Maximum compliance errors for arbitrary force directions for *quasi-serial manipulator*

Figure 3. Maximum compliance errors for arbitrary force direction for serial (a) and quasi-serial (b) manipulators

Summarizing the above case study results dealing with a particular case study, it is possible to define several research problems that are in the focus of this paper:

(i) development of manipulator selection methodology using compliance maps and optimal task placement technique;

(ii) boundary definition between technological tasks which suit in the best way for serial and quasi-serial architectures;

(iii) analysis of existing manipulators from point of view of their stiffness properties and their suitability for typical technological tasks.

To demonstrate the proposed methodology utility, it is also reasonable to apply it to a particular industrial problem, which will be presented in Section IV.

III. Influence of Manipulator Architecture on Machining Accuracy

A. Evaluation of manipulator stiffness properties

Obviously, we cannot evaluate manipulator performance with respect to machining through elastic or geometrical properties only: an appropriate performance measure should take into account also external force/torque directions and magnitudes. The problem becomes more complicated if external actions are not given. In this case, it is reasonable to consider all possible directions of external loading and to estimate maximal compliance errors in the work-point:

$$\rho_p = \max_{\varphi_i} \left| \mathbf{k}_C \cdot \mathbf{F} \cdot \mathbf{R}(\boldsymbol{\varphi}_i) \right|; \qquad \boldsymbol{\varphi}_i \in [-\boldsymbol{\pi}, \boldsymbol{\pi}] \qquad (1)$$

where $\mathbf{k}_C = \mathbf{J}(\mathbf{q}) \cdot \mathbf{k}_\theta \cdot \mathbf{J}(\mathbf{q})^T$ is the manipulator compliance for configuration $\mathbf{q}$, $\mathbf{F}$ is an external loading applied to the manipulator end-effector, $\mathbf{R}(\boldsymbol{\varphi}_i)$ is the rotation matrix allowing us to estimate compliance errors for any force direction $\boldsymbol{\varphi}_i$, $\mathbf{J}(\mathbf{q})$ is Jacobian matrix and matrix $\mathbf{k}_\theta = diag(k,k)$ collects joint compliances k.

In practice, the direction of maximal and minimal compliance errors can be obtained via singular value decomposition of the compliance matrix $\mathbf{k}_C = \mathbf{U} \cdot \sum \cdot \mathbf{V}^T$, where the diagonal matrix $\sum = diag(\sigma_{\max}, ..., \sigma_{\min})$ contains singular values, $\mathbf{U}$ and $\mathbf{V}$ are orthogonal matrices that in this particular case are equal, i.e. $\mathbf{U} = \mathbf{V}$ (since the compliance matrix $\mathbf{k}_C$ is always symmetrical). The first line of matrix $\mathbf{V}$ defines the direction in which the manipulator in configuration $\mathbf{q}$ provides the minimum resistance to the external loading, i.e. the force direction that causes the maximum end-effector compliance error. Similarly, the last line of matrix $\mathbf{V}$ defines the strongest direction, i.e. the direction in which the manipulator is less sensitive to the external loading. Corresponding values of $\sigma_{\max}, ..., \sigma_{\min}$ define the magnitude of compliance errors and ratio between them allows a user to compare manipulator compliance in different directions. Hence, values $\sigma_{\max}$ will be used to estimate manipulator stiffness properties in the given configuration $\mathbf{q}$.

It is worth mentioning that manipulator architecture analysis cannot be performed in a single point since the majority of technological process cannot be performed using a single work-point. For this reason, let us define *benchmark tasks,* which will be used further to estimate manipulators performances. Obviously, it is not possible to define a single benchmark task that covers the majority of machining operations, and thus we consider three task types:

Task A: *Isotropic-shape tasks*, which can be circumscribed by a circle S of the radius d;

Task B: *Quasi-isotropic shape tasks* with a moderate spread, which can be placed in the rectangular zone of the size $S = \{2d \times d\}$;

Task C: *Extended-shape tasks*, which can be placed in a wide rectangular zone of the size $S = \{10d \times d\}$.

While such benchmark tasks may provide a very rough approximation for some complex tasks, they allow to classify all technological tasks into the typical groups and to analyze the manipulator performance for the group of tasks that meet certain requirements. Independently of the considered case, it is reasonable to evaluate the manipulator performance using maximum compliance error within the benchmark task zone

$$\rho_S = \max_{\mathbf{q}} \{ \sigma_{max}(\mathbf{q}) \mid g(\mathbf{q}) \in S \} \qquad (2)$$

where the function $g(\mathbf{q})$ defines the manipulator geometry (direct kinematics), and S is the corresponding task workspace area. Further, we refer this performance measure as the robot benchmark task accuracy (RBTA). Using this performance measure it is possible to estimate potential compliance errors caused by the tool-workpiece interaction and to compare potential accuracy of different manipulators for the same type of technological tasks. In fact, the product $\rho_S \cdot |\mathbf{F}|$ defines the guaranteed accuracy of robot-based machining if the cutting force does not overcome $|\mathbf{F}|$ and if the workpiece is placed inside of optimally located benchmark zone S within the robot workspace.

To analyze the potential of each of the manipulator architecture, it is also required to address the impact of link lengths ratio μ, which directly effects Jacobian matrices and the Cartesian stiffness matrix. In practice, this ratio usually varies from 0.8 to 1.2. We extend this interval to the range of 0.5...1.5 in order to consider the problem wider.

B. Comparison of serial and quasi-serial architectures

To compare manipulators performance for different benchmark tasks let us compute and evaluate the error maps within the robot workspace using expression (2) and varying the benchmark task S size and location. For the error maps evaluation, the optimal task placement technique is used

$$[\mathbf{p}_0^*, \rho_S^*] = \arg\left[\min_{\mathbf{p}_0} \max_{\mathbf{q}} \left\{\sigma_{max}(\mathbf{q}) \mid g(\mathbf{q}) \in S(\mathbf{p}_0, d)\right\}\right] \quad (3)$$

which provides the best task location $\mathbf{p}_0^*$ (among all possible $\mathbf{p}_0$) and corresponding accuracy ρ_S^* for each given task size d. It should be noted that both for serial and quasi-serial manipulators the compliance errors do not depend on angle q_2 (Fig. 2 and Fig. 3). It means that for *isotropic-shape tasks* (Task A) the problem of the optimal task placement and accuracy evaluation reduces to a one-dimensional search with respect to q_3. Relevant algorithm allows us to define the optimal task placement and to evaluate manipulator accuracy. Applying it to the serial and quasi-serial manipulators, we computed values of benchmark accuracy ε_S for different task size d and different link lengths ratio $\mu = l_3 / l_2$ (assuming that $l_2 + l_3 = const$, and all stiffness coefficients are equal). Figure 4 presents simulation results, which allow to compare potential accuracy for both architectures. As follows from them, for the *quasi-serial manipulator*, the best positioning accuracy is achieved for the link length ratio $\mu = 1.0$ and it does not depend on task size d. Moreover, the manipulator with such ratio may perform maximum size tasks compared to the quasi-serial manipulators with $\mu > 1.0$ and $\mu < 1.0$. In contrast, for the *serial manipulator*, the optimal link length ratio depends on the task size. In particular, for small tasks with $d/(l_2 + l_3) < 0.25$ it is preferable to have link length ratio $\mu = 0.7$ while for large tasks with $d/(l_2 + l_3) > 0.4$ the optimal ratio is $\mu = 1.0$. For reader's convenience, optimal values of μ are highlighted in Fig. 4 with red lines.

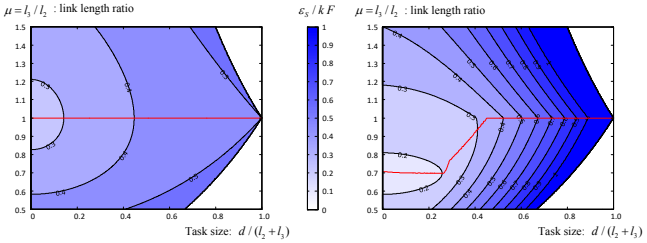

(a) *Case of the quasi-serial manipulator* (b) *Case of the serial manipulator*

Figure 4. Normalised accuracy ε_S / kF for the isotropic-shape case

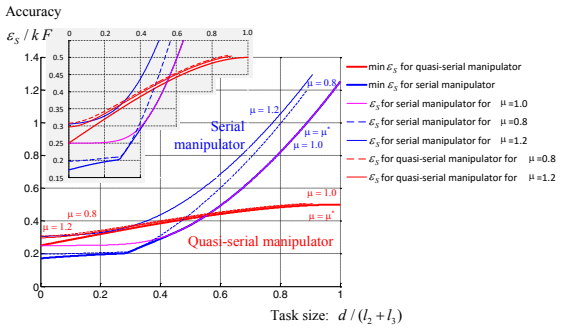

Figure 5. Accuracy for serial and quasi-serial manipulators (Task A)

To make the comparison of two architectures more evident, Fig. 5 presents potential accuracy for the isotropic-shape tasks that is achieved for different link-length ratios μ. The latter includes the optimal value of $\mu = \mu^*$ as well as $\mu = 0.8, 1.0, 1.2$ that are widely used in practice. The results show that for small isotropic-shape tasks the serial manipulators are preferable since they are able to ensure better accuracy. On the other hand, the quasi-serial manipulators better suit for a rather large task size, i.e. $d/(l_2 + l_3) > 0.55$. Besides, the quasi-serial manipulators provide similar performance for both small and large tasks while the properties of their serial counterparts essentially depend on the task size. It should be also emphasized that the link length ratio in the range $\mu \in [0.8; 1.2]$ does not affect essentially a quasi-serial manipulator accuracy. On the contrary, the serial manipulator is very sensitive to proper selection of the link length ratio μ; for the above considered range of $\mu \in [0.8; 1.2]$ a serial manipulator accuracy may be twice as worse compared to the minimum value.

In the case of *quasi-isotropic task* (Task B) and *extended-shape shape task* (Task C), the problem of the optimal task placement and accuracy evaluation is a two-dimensional one with respect to *x* and *y*. Here, taking into account that the error maps are composed of concentric circles (Fig. 3), it is sufficient to check accuracy for the rectangle vertices only. Thus, it is reasonable to fix the task orientation with respect to one of the Cartesian axes. Hence, the optimal task placement is always symmetric with respect to these axes, which allows us to apply a one-dimensional search while considering both horizontal and vertical task orientations.

Applying corresponding optimization algorithm, there were computed values of the benchmark accuracy ε_S for different task size $a \times b$ and different link lengths ratio $\mu = l_3 / l_2$ (for both serial and quasi-serial manipulators). For the quasi-isotropic case $d \times 2d$ (Task B), simulation results are presented in Fig. 6. Figure 7 presents potential accuracy that is achieved for different link-length ratios μ, including the optimal value of $\mu = \mu^*$ as well as $\mu = 0.8, 1.0, 1.2$. Similar to the previous case, for Task B a quasi-serial manipulator best positioning accuracy is achieved for link length ratio $\mu = 1.0$ (i.e. for equal links $l_2 = l_3$). For a serial manipulator, optimal link-length ration is $\mu = 0.65$ for small tasks and $\mu = 1.0$ for large-dimensional tasks. It is also worth mentioning that for a quasi-serial manipulator positioning accuracy does not vary essentially with variation of link length ratio μ and task dimensions. However, limits on the task dimensions highly depend on the link length ratio. In particular, commonly used manipulators with $\mu = 0.8$ and $\mu = 1.2$ may perform tasks with the size up to $d/(l_2 + l_3) = 0.4$, while a manipulator with $\mu = 1.0$ can be used for tasks with the size up to $d/(l_2 + l_3) = 0.7$. In contrast, serial manipulators are less constrained by link length ratio in terms of maximum task size. In addition, they ensure higher accuracy for small size tasks. Nevertheless, for relatively large tasks with $d/(l_2 + l_3) > 0.3$ serial manipulators are less competitive (Fig. 7). Hence, for small quasi-isotropic-shape tasks, serial manipulators are preferable since they are able to ensure higher accuracy. While for large tasks quasi-serial manipulators with link length ratio $\mu = 1.0$ ensure the best performance.

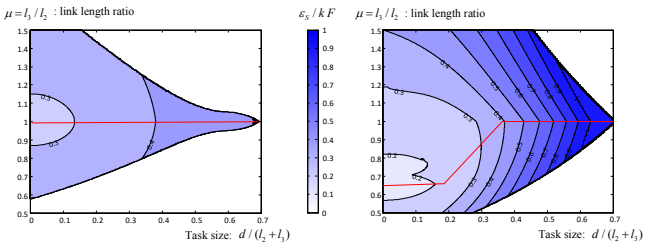

(a) *Case of the quasi-serial manipulator* (b) *Case of the serial manipulator*

Figure 6. Normalised accuracy $\varepsilon_S / k F$ for quasi-isotropic-shape case

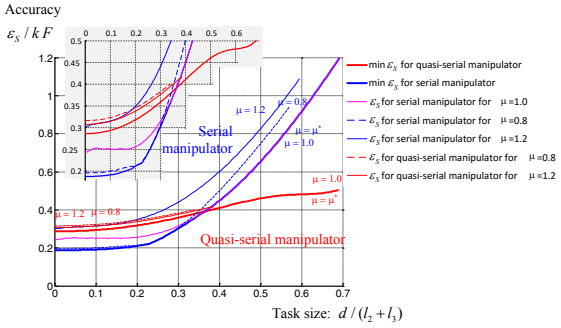

Figure 7. Accuracy for serial and quasi-serial manipulators (Task B)

Similar plots were obtained for the extended shape case (Task C, $d \times 10d$), they are presented in Fig. 8 and Fig. 9. These results confirm discovered above general tendency for Tasks A and B. However, here serial manipulators can be used for essentially larger tasks. Thus, for Task C quasi-serial manipulators are preferable, while their optimal link length ratio highly depends on the task size and varies from 0.55 to 1.0.

The results of this study for all considered tasks are summarized in Table 1, which shows accuracy limits and preferred manipulators for Tasks A, B and C. As follows from them, a serial manipulator is preferable for small-size task, and in this case the optimal link length ratio is $\mu = 0.65...0.70$. The particularity of serial robots is that their accuracy highly depends on the machining task size. In contrast, quasi-serial manipulators provide almost the same accuracy for all tasks, assuming that the task is optimally located. For large-size tasks, quasi-serial manipulators are preferable, their optimal link length ratio is $\mu = 1.0$.

We emphasize that the above presented results do not consider the joint limits because our objective was to find physical limits of serial and quasi-serial architectures and to compare them for a general case. The following Section takes this issue into account.

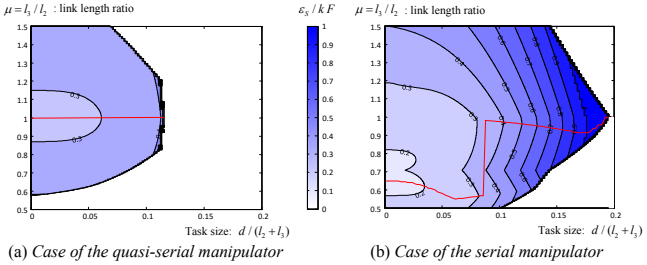

(a) *Case of the quasi-serial manipulator* (b) *Case of the serial manipulator*

Figure 8. Normalised accuracy $\varepsilon_S / k F$ for the extended-shape case

TABLE I. ACCURACY OF SERIAL AND QUASI-SERIAL MANIPULATORS

Normalized accuracy, $\varepsilon_S / k F$								
Task dim.	0.1		0.3		0.5		0.8	
μ	SM	QSM	SM	QSM	SM	QSM	SM	QSM
Isotropic-shape task, d								
0.8	0.20	0.32	0.21	0.37	0.45	0.43	1.00	0.49
1.0	0.25	0.28	0.26	0.35	0.37	0.42	0.82	0.48
1.2	0.31	0.31	0.36	0.37	0.55	0.43	1.05	0.49
Min.	0.18	0.28	0.20	0.35	0.37	0.42	0.82	0.48
Quasi-isotropic-shape task, $d \times 2d$								
0.8	0.20	0.33	0.30	0.38	0.75	-	-	-
1.0	0.25	0.29	0.32	0.36	0.65	0.46	-	-
1.2	0.32	0.32	0.44	0.38	0.82	-	-	-
Min.	0.19	0.29	0.30	0.36	0.65	0.46	-	-
Extended-shape task, $d \times 10d$								
0.8	0.43	0.38	-	-	-	-	-	-
1.0	0.38	0.36	-	-	-	-	-	-
1.2	0.48	0.38	-	-	-	-	-	-
Min.	0.38	0.36	-	-	-	-	-	-

SM – Serial manipulator ***QSM*** – Quasi-serial manipulator

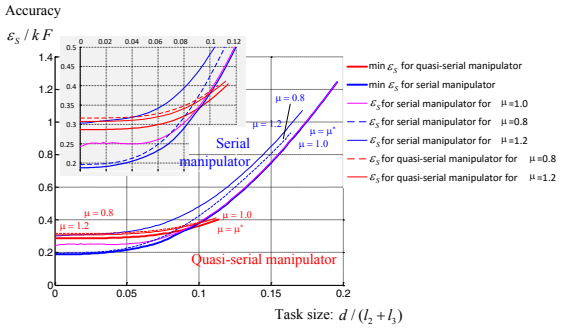

Figure 9. Accuracy for serial and quasi-serial manipulators (Task C)

IV. APPLICATION EXAMPLE: RANKING OF TYPICAL COMMERCIALLY AVAILABLE INDUSTRIAL ROBOTS

Let us apply the developed technique to the comparative analysis of typical serial and quasi-serial manipulators. The considered set contains 10 industrial robots from different manufacturers with a payload of about 200 kg. The manipulator performances were compared for isotropic, quasi-isotropic and extended tasks. The list of the examined robots is given in Table 2, which also provides architecture type, principal geometric parameters and nominal payload. The comparison analysis was performed under the following assumptions:

- Robot compliances are concentrated in the actuated joints;
- All examined robots have the same stiffness parameters, equal for all actuated joints (10^{-6} rad/Nm, typical value for heavy industrial robots);
- The external loading magnitude is the same for all robots (1.0 kN, i.e. about 50% of payload), while its direction is not defined and the worst case must be considered;
- For each case study, realistic joint limits from manufacturer's datasheets are considered;

- The manipulator accuracy is estimated for benchmark Tasks A, B and C that are optimally located within the robot workspace (either vertically or horizontally).

These assumptions allow us to compare manipulator architecture (serial vs. quasi-serial) without focusing on exact actuator parameters, which in reality differ from one robot to another.

TABLE II. EXAMINED INDUSTRIAL ROBOTS AND THEIR PARAMETERS

Robot	Architecture	μ	Working radius	Payload
Yaskawa ES200RD II	S	0.92	3.140 m	200 kg
Yaskawa HP350D-200	QS	0.57	3.036 m	200 kg
ABB IRB 6650S-200	S	1.10	3.039 m	200 kg
ABB IRB 6400 2.4-200	QS	0.89	2.400 m	200 kg
KUKA KR210	S	0.96	2.700 m	210 kg
Stäubli TX340 SH	QS	0.80	3.450 m	165 kg
Fanuc R-2000iC/210R	S	0.83	3.095 m	210 kg
Fanuc M-900iA/200P	QS	0.61	3.507 m	200 kg
Kawasaki BT200L	S	0.91	3.151 m	200 kg
Kawasaki ZX200U	QS	0.83	2.650 m	200 kg

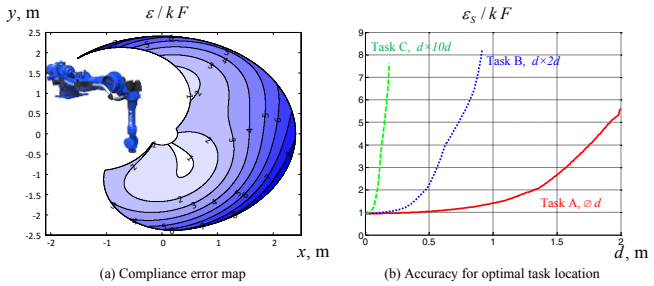

(a) Compliance error map (b) Accuracy for optimal task location

Figure 10. Normalised accuracy of a serial architecture equivalent to the industrial robot Yaskawa ES200RD II

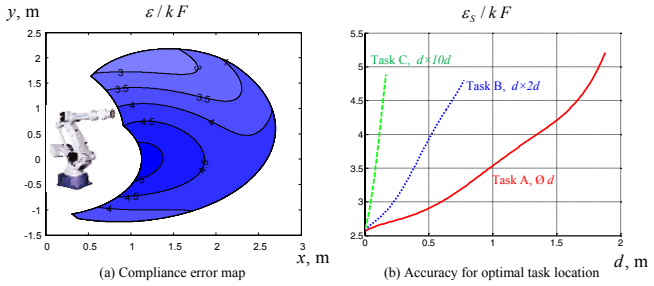

(a) Compliance error map (b) Accuracy for optimal task location

Figure 11. Normalised accuracy of a quasi-serial architecture equivalent to the industrial robot Yaskawa HP350D-200

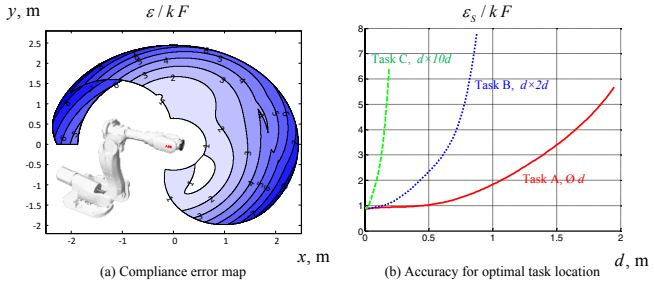

(a) Compliance error map (b) Accuracy for optimal task location

Figure 12. Normalised accuracy of a serial architecture equivalent to the industrial robot ABB IRB 6650S-200

The comparison study results are presented in Fig. 10-19. For each examined manipulator the figure contains the compliance error map and the best accuracy for the considered tasks. The obtained maps show the worst-case compliance errors in workspace points corresponding to the most adverse force direction. Because of normalization and accepted stiffness coefficients, the presented errors can be also treated as the end-effector deflections (in mm) under the external loading of 1.0 kN. The right-hand plots show the worst-case compliance errors for the area corresponding to the benchmark tasks, which is assumed to be optimally located within the robot workspace. In addition, they allow a user to evaluate the maximum task size that can be placed within the workspace taking into account robot geometry and joint limits. For instance, Fig. 13 points out that for the quasi-serial architecture corresponding to ABB IRB 6400 manipulator, the best normalized accuracy in a single point is about 1.26, while for quasi-isotropic task of size 0.5×1.0 the best achievable value is essentially higher and is equal to 2.68. Integrated summary of the obtained results is presented in Table 3.

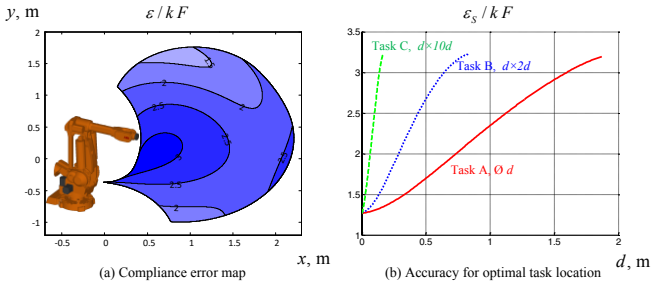

(a) Compliance error map (b) Accuracy for optimal task location

Figure 13. Normalised accuracy of a quasi-serial architecture equivalent to the industrial robot ABB IRB 6400 2.4-200

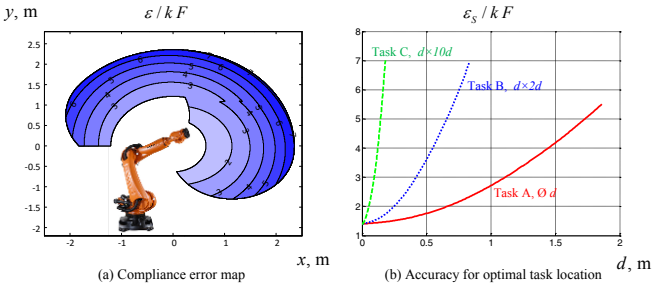

(a) Compliance error map (b) Accuracy for optimal task location

Figure 14. Normalised accuracy of a serial architecture equivalent to the industrial robot KUKA KR210

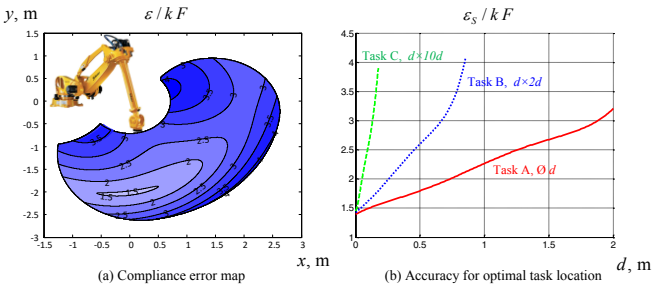

(a) Compliance error map (b) Accuracy for optimal task location

Figure 15. Normalised accuracy of a quasi-serial architecture equivalent to the industrial robot Stäubli TX340 SH

The obtained results allow us to make the following conclusions:

Serial manipulators are preferable for small and medium tasks. In particular, for Task A of size 0.1 m (isotropic task) a serial architecture allows to ensure the normalized error of ε_s =0.90 mm while the best value for a quasi-serial architecture is equal to 1.24 mm. Similarly, for Task B of size 0.1×0.2 m (quasi-isotropic task) the best value for a serial architecture is 0.97 mm in contrast to 1.36 mm for a quasi-serial one.

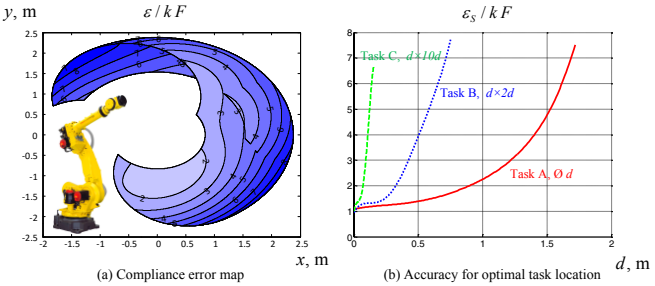

(a) Compliance error map (b) Accuracy for optimal task location

Figure 16. Normalised accuracy of a serial architecture equivalent to the industrial robot Fanuc R-2000iC/210R

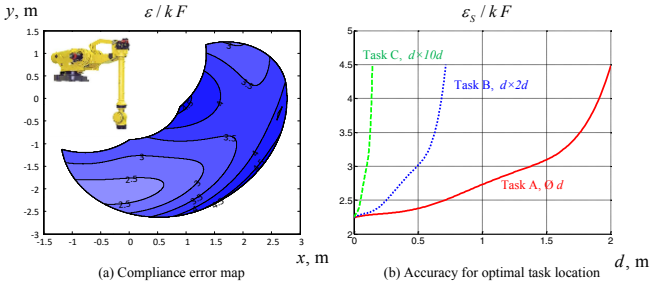

(a) Compliance error map (b) Accuracy for optimal task location

Figure 17. Normalised accuracy of a quasi-serial architecture equivalent to the industrial robot Fanuc M-900iA/200P

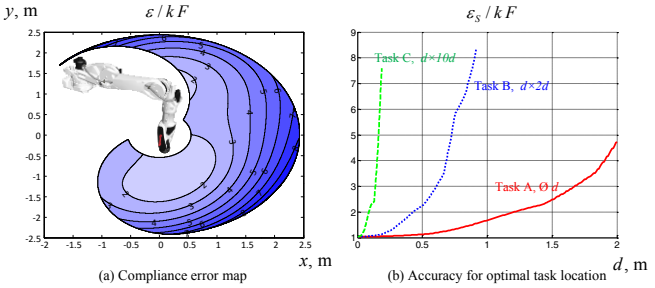

(a) Compliance error map (b) Accuracy for optimal task location

Figure 18. Normalised accuracy of a serial architecture equivalent to the industrial robot Kawasaki BT200L

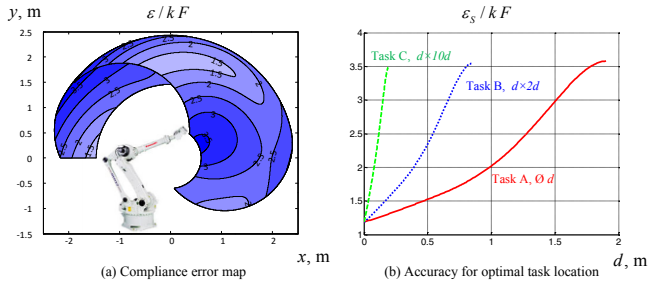

(a) Compliance error map (b) Accuracy for optimal task location

Figure 19. Normalised accuracy of a quasi-serial architecture equivalent to the industrial robot Kawasaki ZX200U

Quasi-serial manipulators are preferable for large tasks. For instance, for Task C of size 0.15×1.5 m (extended) a quasi-serial architecture allows us to ensure the normalized error ε_s =2.94 mm while the best value for a serial architecture is equal to 3.93 mm. However, in some cases a large task cannot be located in the manipulator workspace because of specific joint limits of a quasi-serial architecture.

TABLE III. NORMALISED ACCURACY OF SERIAL AND QUASI-SERIAL MANIPULATORS FOR DIFFERENT TASKS

Task Type	**Task A, Ø d**		**Task B, d×2d**		**Task C, d×10d**	
d, m	**0.1**	**1.0**	**0.1**	**0.5**	**0.05**	**0.15**
Yaskawa ES200RD II	0.95	1.40	0.97	2.24	1.10	5.00
Yaskawa HP350D	2.64	3.53	2.75	3.93	3.06	4.65
ABB IRB 6650S	0.90	1.90	0.95	2.23	1.25	3.99
ABB IRB 6400	1.31	2.35	1.42	2.67	1.79	3.13
KUKA KR210	1.43	2.72	1.53	3.61	1.99	5.37
Stäubli TX340 SH	1.49	2.25	1.63	2.63	1.98	3.35
Fanuc 2000iC/210R	1.16	2.22	1.24	4.08	1.62	6.60
Fanuc M-900iA/200P	2.27	2.72	2.31	3.04	2.50	-
Kawasaki BT200L	1.04	1.68	1.06	2.26	1.27	3.93
Kawasaki ZX200U	1.24	2.00	1.36	2.31	1.67	3.05
min ε_s	0.90	1.40	0.97	2.23	1.10	3.05

It is worth mentioning that these conclusions well agree with the results of Section III that deal with the normalized manipulator geometry: serial manipulators are preferable for small and medium size tasks, quasi-serial manipulators are competitive for medium size tasks and advantageous for large size tasks. However, in practice the workspace of quasi-serial manipulators is more constrained by joint limits, which sometimes do not allow to locate some large-size tasks that are acceptable for serial manipulators. It should be also emphasized that serial manipulators accuracy is rather sensitive to the task location, while the quasi-serial architecture provides more homogeneous compliance error properties with respect to the task position in the robot workspace.

V. CONCLUSIONS

The paper proposes a new methodology for industrial robot comparison and ranking with respect to the accuracy in machining application. Particular attention is paid to capability evaluation of serial and quasi-serial architectures. The developed technique is based on estimation of the maximum compliance error caused by machining force. For each end-effector location, the weakest direction with respect to external loading is evaluated via singular value decomposition of the Cartesian stiffness matrix. Three benchmark tasks covering the majority of technological processes are used to compare the robot accuracy under the loading. To estimate full potential of each architecture, the optimal task placement technique is used to locate optimally the workpiece within the robot workspace. The developed methodology was applied both to general comparison study of serial and quasi-serial manipulators and to the case study dealing with the comparison analysis of 10 particular serial and quasi-serial industrial robots from different manufactures.

The obtained results show that quasi-serial manipulators are preferable for large-dimensional tasks, while serial ones better suit small and medium size tasks, provided that the task is optimally located within the workspace. When the task location cannot be optimized, quasi-serial manipulators should be used since they provide more homogenous compliance error distribution. Another advantage of quasi-serial manipulators is related to the fact that the best accuracy is ensured in the middle of the workspace, while the minimum of the compliance errors for serial manipulators is achieved on the workspace boundary.

As a part of our future work we will enhance the developed methodology by taking into account specific particularities of considered machining technology. Besides, it will be applied to comparison analysis of wider set of existing industrial robots and for task-oriented design of new industrial robots.

ACKNOWLEDGMENT

The work presented in this paper was partially funded by Innopolis University and project FEDER ROBOTEX, France.

REFERENCES

[1] F. Pierrot, V. Nabat, O. Company, S. Krut, and P. Poignet, "Optimal Design of a 4-DOF Parallel Manipulator: From Academia to Industry," *Robotics, IEEE Transactions on,* vol. 25, pp. 213-224, 2009.

[2] M. Terrier, A. Dugas, and J.-Y. Hascoët, "Qualification of parallel kinematics machines in high-speed milling on free form surfaces," *International Journal of Machine Tools and Manufacture,* vol. 44, pp. 865-877, 6// 2004.

[3] M. Chérif, H. Thomas, B. Furet, and J.-Y. Hascoët, "Generic modelling of milling forces for CAD/CAM applications," *International Journal of Machine Tools and Manufacture,* vol. 44, pp. 29-37, 1// 2004.

[4] G.-C. Vosniakos and E. Matsas, "Improving feasibility of robotic milling through robot placement optimisation," *Robotics and Computer-Integrated Manufacturing,* vol. 26, pp. 517-525, 10// 2010.

[5] N. Mendes, P. Neto, M. A. Simão, A. Loureiro, and J. N. Pires, "A novel friction stir welding robotic platform: welding polymeric materials," *The International Journal of Advanced Manufacturing Technology,* pp. 1-10, 2014.

[6] M. Guillo and L. Dubourg, "Impact & improvement of tool deviation in friction stir welding: Weld quality & real-time compensation on an industrial robot," *Robotics and Computer-Integrated Manufacturing,* vol. 39, pp. 22-31, 6// 2016.

[7] W. Zhu, W. Qu, L. Cao, D. Yang, and Y. Ke, "An off-line programming system for robotic drilling in aerospace manufacturing," *The International Journal of Advanced Manufacturing Technology,* vol. 68, pp. 2535-2545, 2013.

[8] T. Olsson, M. Haage, H. Kihlman, R. Johansson, K. Nilsson, A. Robertsson*, et al.*, "Cost-efficient drilling using industrial robots with high-bandwidth force feedback," *Robotics and Computer-Integrated Manufacturing,* vol. 26, pp. 24-38, 2// 2010.

[9] Y. Guo, H. Dong, G. Wang, and Y. Ke, "Vibration analysis and suppression in robotic boring process," *International Journal of Machine Tools and Manufacture,* vol. 101, pp. 102-110, 2// 2016.

[10] B. Denkena and T. Lepper, "Enabling an Industrial Robot for Metal Cutting Operations," *Procedia CIRP,* vol. 35, pp. 79-84, // 2015.

[11] A. Klimchik, A. Pashkevich, D. Chablat, and G. Hovland, "Compliance error compensation technique for parallel robots composed of non-perfect serial chains," *Robotics and Computer-Integrated Manufacturing,* vol. 29, pp. 385-393, 4// 2013.

[12] N. R. Slavkovic, D. S. Milutinovic, and M. M. Glavonjic, "A method for off-line compensation of cutting force-induced errors in robotic machining by tool path modification," *The International Journal of Advanced Manufacturing Technology,* vol. 70, pp. 2083-2096, 2013.

[13] G. Alici and B. Shirinzadeh, "A systematic technique to estimate positioning errors for robot accuracy improvement using laser interferometry based sensing," *Mechanism and Machine Theory,* vol. 40, pp. 879-906, 8// 2005.

[14] P. Drouet, S. Dubowsky, S. Zeghloul, and C. Mavroidis, "Compensation of geometric and elastic errors in large manipulators with an application to a high accuracy medical system," *Robotica,* vol. 20, pp. 341-352, 2002.

[15] B. Shirinzadeh, P. L. Teoh, Y. Tian, M. M. Dalvand, Y. Zhong, and H. C. Liaw, "Laser interferometry-based guidance methodology for high precision positioning of mechanisms and robots," *Robotics and Computer-Integrated Manufacturing,* vol. 26, pp. 74-82, 2// 2010.

[16] A. Klimchik, Y. Wu, C. Dumas, S. Caro, B. Furet, and A. Pashkevich, "Identification of geometrical and elastostatic parameters of heavy industrial robots," in *IEEE International Conference on Robotics and Automation (ICRA)* 2013, pp. 3707-3714.

[17] J. Belchior, M. Guillo, E. Courteille, P. Maurine, L. Leotoing, and D. Guines, "Off-line compensation of the tool path deviations on robotic machining: Application to incremental sheet forming," *Robotics and Computer-Integrated Manufacturing,* vol. 29, pp. 58-69, 8// 2013.

[18] C. Dumas, S. Caro, M. Cherif, S. Garnier, and B. Furet, "Joint stiffness identification of industrial serial robots," *Robotica,* vol. 30, pp. 649-659, 2012.

[19] A. Klimchik, B. Furet, S. Caro, and A. Pashkevich, "Identification of the manipulator stiffness model parameters in industrial environment," *Mechanism and Machine Theory,* vol. 90, pp. 1-22, 8// 2015.

[20] K. Subrin, L. Sabourin, R. Cousturier, G. Gogu, and Y. Mezouar, "New Redundant Architectures in Machining: Serial and Parallel Robots," *Procedia Engineering,* vol. 63, pp. 158-166, // 2013.

[21] B. Vemula, G. Spampinato, T. Brogardh, and X. Feng, "Stiffness Based Global Indices for Structural Evaluation of Anthropomorphic Manipulators," in *ISR/Robotik 2014; 41st International Symposium on Robotics; Proceedings of*, 2014, pp. 1-8.

[22] C. Gosselin and J. Angeles, "Global performance index for the kinematic optimization of robotic manipulators," *Journal of mechanisms, transmissions, and automation in design,* vol. 113, pp. 220-226, 1991.

[23] T. Yoshikawa, "Manipulability of robotic mechanisms," *International Journal of Robotics Research,* vol. 4, pp. 3-9, 1985.

[24] B. Bounab, "Multi-objective optimal design based kineto-elastostatic performance for the DELTA parallel mechanism," *Robotica,* vol. 34, pp. 258-273, 2016.

[25] Y. Sun and J. M. Hollerbach, "Observability index selection for robot calibration," in *Robotics and Automation, 2008. ICRA 2008. IEEE International Conference on*, 2008, pp. 831-836.

[26] J. Imoto, Y. Takeda, H. Saito, and K. Ichiryu, "Optimal kinematic calibration of robots based on maximum positioning-error estimation (Theory and application to a parallel-mechanism pipe bender)," in *Computational Kinematics*, ed: Springer, 2009, pp. 133-140.

[27] Y. Wu, A. Klimchik, S. Caro, B. Furet, and A. Pashkevich, "Geometric calibration of industrial robots using enhanced partial pose measurements and design of experiments," *Robotics and Computer-Integrated Manufacturing,* vol. 35, pp. 151-168, 10// 2015.

[28] S. J. Yan, S. K. Ong, and A. Y. C. Nee, "Stiffness analysis of parallelogram-type parallel manipulators using a strain energy method," *Robotics and Computer-Integrated Manufacturing,* vol. 37, pp. 13-22, 2// 2016.

[29] A. Klimchik, D. Chablat, and A. Pashkevich, "Stiffness modeling for perfect and non-perfect parallel manipulators under internal and external loadings," *Mechanism and Machine Theory,* vol. 79, pp. 1-28, 9// 2014.

[30] S.-i. Matsuoka, K. Shimizu, N. Yamazaki, and Y. Oki, "High-speed end milling of an articulated robot and its characteristics," *Journal of Materials Processing Technology,* vol. 95, pp. 83-89, 10/15/ 1999.

[31] A. Klimchik, A. Pashkevich, Y. Wu, S. Caro, and B. Furet, "Design of calibration experiments for identification of manipulator elastostatic parameters," *Applied Mechanics and Materials,* vol. 162, pp. 161-170, 2012.